行政院國家科學委員會專題研究計畫　成果報告

臭氧現地處理法復育土壤中之非水相液體之應用及模擬

計畫類別：個別型計畫
計畫編號：NSC94-2211-E-041-015-
執行期間：94 年 08 月 01 日至 95 年 07 月 31 日
執行單位：嘉南藥理科技大學環境工程與科學系(所)

計畫主持人：宋孟浩
共同主持人：陳煜斌，李孫榮
計畫參與人員：余哲民，陳必祥

報告類型：精簡報告

處理方式：本計畫可公開查詢

中　華　民　國 95 年 10 月 25 日

Remediation of Non-Aqueous Phase Liquid in Soils by In-Situ Ozonation

Abstract

NAPL contamination remains a serious problem today. The soil ozonation method offers a promising alternative for LNAPL remediation. In this study, a mathematical model to describe interactions of multi components in a multi-phase system was developed. The model was scaled so that important parameters pertinent to the process were determined. Column profiles and breakthrough curves under various controlling conditions were simulated to understand how these systems can be optimized. Laboratory soil column experiments exemplified by toluene were also conducted to mimic the release of gasoline in the vadose zone. Operations of ozone injection were compared to nitrogen purging. Also, effects of ozone flow rate and toluene mass were investigated.

摘要

非水相液體的汙染，至今仍然是一個嚴重的問題。以臭氧處理法來處理土壤中的這類較輕的非水相液體污染物質，是一很有潛力的方法。本研究發展出一個可以用來描述多種物質，位於多個不同相之間的互動反應模式。當選擇適當之參數將該模式無因次化後，我們可以從其中決定重要之控制參數，並進而將該系統最佳化。管柱剖面以及各種物質土壤之穿透曲線，皆可由模擬中得到。本研究實驗上以汽油中之主要成分物之一的甲苯液體，作為土壤之污染物，以測試臭氧處理法與氮氣沖提法之效果差異，並研究臭氧通氣流量與甲苯之含量對處理效率之提升程度。

I. Introduction

Accidental spill of nonaqueous phase liquid (NAPL) such as fuel, petroleum products, and chlorinated hydrocarbon solvents has caused serious soil contamination problems worldwide (Khachikian and Harmon 2000). These NAPL compounds have low water solubility, and thus serve as long-term sources of groundwater contamination (Mercer 1990). When released in the unsaturated zone, NAPLs travel downward and laterally toward the water table. Once reaching the water table, light NAPLs (LNAPLs) have the tendency to pool on the phreatic surface and dense NAPLs (DNAPLs) can continue to move downward to be trapped in the saturated soil medium. Therefore, NAPLs can contaminate both unsaturated and saturated subsurface once it is released to the soils.

In-situ air sparging (IAS) coupled with the soil vapor extraction (SVE) method has been a popular remediation alternative to clean up NAPL contaminants (Rogers and Ong 2000). In the SVE operation, a vacuum is induced in the unsaturated zone and thus volatile NAPLs are introduced into the air flow passing through the contaminated zone and removed from soils. In order to further extend the SVE process to remediate non-volatile compounds, a new process called soil ozonation has been developed (Sung and Huang 2002; Yoon, Kim et al. 2002; Shin, Garanzuay et al. 2004). By injecting ozone gas into the SVE system, a faster removal rate can be achieved and no off-gas treatment units will be needed. This has greatly improved the traditional SVE system. However, past studies mainly focus on the application of soil ozonation on non-NAPLs, very few studies concentrate on NAPLs. As a result, the goal of this investigation concentrates on the feasibility study of ozonation of NAPLs in soils, and the development of predictive model for this process.

The local equilibrium assumption (LEA) has been applied to describe mass transfer in some NAPL venting experiments (Hayden, Voice et al. 1994; HO, Liu et al. 1994). However, it was later found that the LEA is limited and thus recently non-equilibrium transport models have been formulated in several applications (Harper, Stiver et al. 2003). To account for chemical reactions occurring in the soil ozonation system, non-equilibrium mass transfer coupled with reaction must be formulated into the model (Sung and Huang 2002; Shin, Garanzuay et al. 2004). Important dimensionless parameters such as Stanton number and Damkohler number have been found to critical in assessment of rate limiting steps during an operation (Sung and Huang 2002). The objectives of this study were to develop mathematical models to describe the soil ozonation of NAPL-contaminated soils, to determine important dimensionless that controls the process, and finally to conduct laboratory experiments to optimize the model.

II. Mathematical models

Governing equations for the VOC gas, NAPL, and ozone are needed to describe the process. The governing equation of the VOC gas (C_g) transport can be written as

$$nS_g \frac{\partial C_g}{\partial t} = -q_g \frac{\partial C_g}{\partial x} + nS_g k_{ga}(C_s - C_g) - nS_g k_r C_g C_z \tag{1}$$

where n is the porosity of the soil, S_g is the degree of gas saturation, q_g is the Darcy velocity of the VOC gas, k_{ga} is the NAPL-gas mass transfer coefficient, k_r is the gas-phase second-order rate constant between ozone and VOC, C_s and C_z represents saturated VOC gas and ozone gas concentrations, respectively. The governing equation for the NAPL compound can be described by the following equation

$$n\rho_o \frac{\partial S_o}{\partial t} = -nS_g k_{ga}(C_s - C_g) \tag{2}$$

where S_o is the degree of NAPL saturation, and ρ_o represents the density of the NAPL. The governing equation of the ozone gas (C_z) can be written as

$$nS_g \frac{\partial C_z}{\partial t} = -q_g \frac{\partial C_z}{\partial x} - \nu nS_g k_r C_g C_z - nS_g k_d C_z \tag{3}$$

where v is the stoichiometric coefficient between ozone and VOC, and k_d represents the first-order self-decomposition constant of ozone.

The NAPL-gas mass transfer coefficient was found to be dependent on the degree of NAPL saturation (S_o), and can be described by the following equation (Yoon et al., 2002)

$$k_{ga} = k_{gai}\left(\frac{S_o}{S_{oi}}\right)^{\beta} \tag{4}$$

where the subscript i represents the initial value, and β is a coefficient ranging from 0.75-0.96. Initial conditions for the above equations (1) to (3) are:

$$C_g(t=0,x) = C_s;\ \ S_o(t=0,x) = S_{oi};\ \ C_z(t=0,x) = 0$$

The left boundary conditions (at x=0) are:

$$C_g(t,x=0) = 0;\ \ S_o(t,x=0) = 0;\ \ C_z(t,x=0) = C_{z0}$$

where C_{z0} is the ozone gas concentration applied at the inlet. The right boundary conditions (at $x=l$) are all subject to zero concentration gradients.

Equations (1) to (3) can be scaled by employing the following new variables:

$$\theta = \frac{C_g}{C_s};\ \ \phi = \frac{S_o}{S_{oi}};\ \ \psi = \frac{C_z}{C_{z0}};\ \ \eta = \frac{x}{l};\ \ \tau = \frac{t}{(l/q_g)}$$

The scaled dimensionless governing equations become

$$nS_g \frac{\partial \theta}{\partial \tau} = -\frac{\partial \theta}{\partial \eta} + St\phi^{\beta}(1-\theta) - Da_1\theta\psi \tag{5}$$

$$\frac{n\rho_o S_{oi}}{C_s}\frac{\partial \phi}{\partial \tau} = -St\phi^{\beta}(1-\theta) \tag{6}$$

$$nS_g \frac{\partial \psi}{\partial \tau} = -\frac{\partial \psi}{\partial \eta} - Da_2\theta\psi - Da_3\psi \tag{7}$$

where *St* is the Stanton's number and equals $(l/v_g)/(1/k_{gai})$, representing the rate of ozone gas convection to mass transfer; Da_1, Da_2, and Da_3 are the Damkohler's number and equal respectively $(l/v_g)/(1/k_r C_{z0})$, $(l/v_g)/(1/\nu k_r C_s)$, and $(l/v_g)/(1/k_d)$, representing the rate of VOC gas convection to chemical reaction with ozone, the rate of ozone gas convection to chemical reaction with VOC, and the rate of ozone gas convection to its self-decomposition. The above equations were solved by the numerical scheme utilizing Crank-Nicolson's central difference method.

III. Experiments

Commercial sands with an average size of 0.31 mm were used for the experiments as pure silica soil materials. Stainless steel columns were used to conduct laboratory experiments. A schematic description of the experimental system is shown in Figure 1 below.

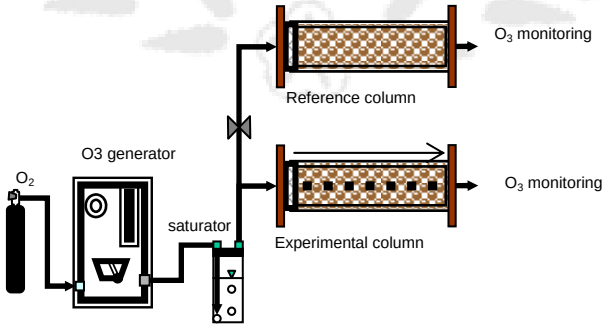

Figure 1. Experimental design of laboratory soil colum,n experiment.

The ozone generator (Model OZ2BTUSL-V/PM) manufactured by Ozotech Inc. (Yreka, CA, USA) was employed to produce ozone from the oxygen tank. Prior to entering the soil column, ozone gas was forced to pass through a saturator filled with $HClO_4$ solution at pH 2.5. Two columns with identical dimensions were connected in parallel. A three-way valve was placed so that ozone can only enter one column at a time. The reference column of soil was prepared following the same procedure as the

experimental column except that no contaminant was spiked. This was to create the same head loss as ozone flowed through. Prior to injecting ozone into the experimental column, the three-way valve was switched to the reference column so that ozone flow rates and concentrations to be applied could be confirmed from the ozone breakthrough curve. Once the desired flow rate and concentration were reached, the three-way valve was switched to the experimental column to start the experiment. Both ozone and VOC gas exiting the column were recorded by UV gas detector (Model T60, PG Instruments Ltd., Leics, United Kingdom) as a function of time.

IV. Results and Discussion

1. Column Profile Simulation of Residues

Figure 2 shows the simulated results of toluene vapor distribution along the column under various times. The *St* and Da_I values in this simulation equals 0.01 and 100, respectively. A small *St* value implies that the rate of NAPL to VOC mass transfer is much smaller than the rate of convective mass transfer, and a large Da_I implies that the rate of chemical reaction is much faster than convective mass transfer. Overall, it demonstrates a condition where various rates have the following sequence: chemical reaction >> convection >> interfacial mass transfer. Under such conditions, VOC is expected to be depleted immediately when ozone is in contact with it. This is evident from results of Figures 2 and 3, where both VOC (θ) and ozone (Ψ) have very narrow reactive zones.

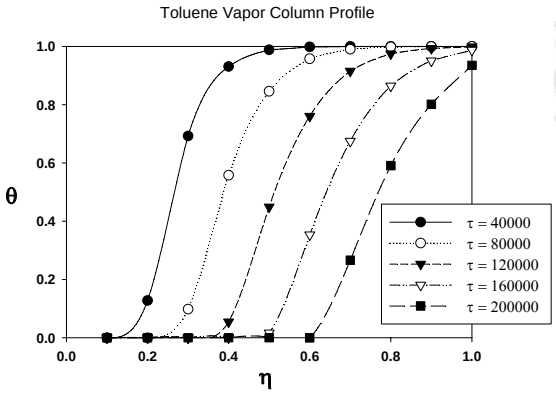

Figure 2. Normalized distribution of toluene vapor in a column when St = 0.01 and Da_I= 100.

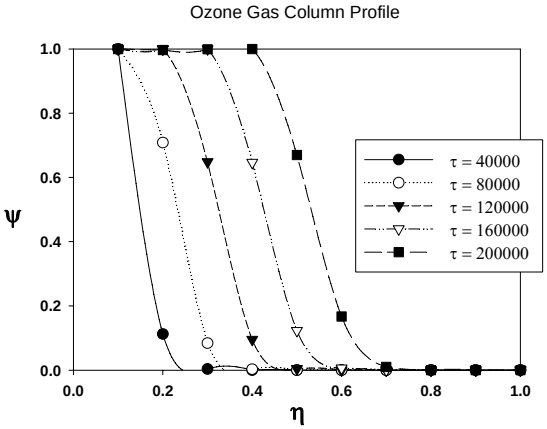

Figure 3. Normalized distribution of ozone gas in a column when St = 0.01, and Da_I= 100.

When the *St* and the Da_I value equals 100 and 0.01, respectively. Different column profiles can be observed as shown in Figures 4 and 5. A large *St* value implies that the rate of NAPL to VOC mass transfer is much faster than the rate of convective mass

transfer, and a small Da_1 implies that the rate of chemical reaction is much slower than convective mass transfer. Overall, it demonstrates a condition where various rates have the following sequence: interfacial mass transfer >> convection >> chemical reaction. Figure 4 indicates that the toluene vapor profiles become independent of reaction times, whereas Figure 5 shows that the ozone gas distribution is strongly dependent on reaction times. In Figure 4, note that the toluene vapor remains nearly saturated when the column length (η) is greater than 0.2 while the ozone gas concentration is dependent on column length at different times. The reason that the VOC can remain saturated is because the rate of mass transfer is so fast that it is replenished in the column immediately after it is consumed. The rate of mass transfer will become slow only when the residual NAPL becomes significantly less. This is what occurs when the length is less than 0.2.

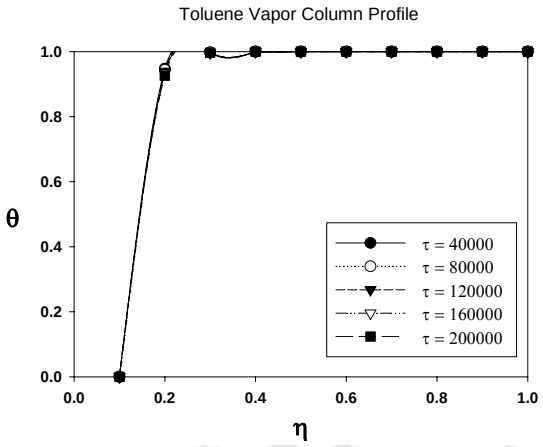

Figure 4. Normalized distribution of toluene vapor in a column when St = 100, and Da_1= 0.01.

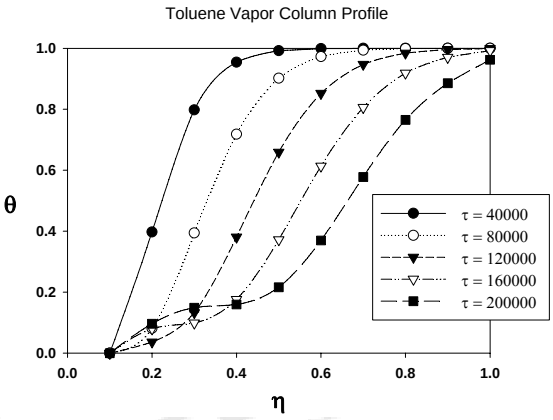

Figure 6. Normalized distribution of VOC in a column when St = 1, and Da_1= 1.

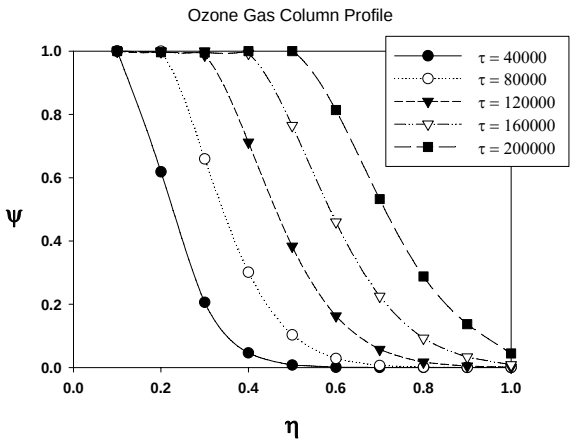

Figure 5. Normalized distribution of ozone gas in a column when St = 100, and Da_1= 0.01.

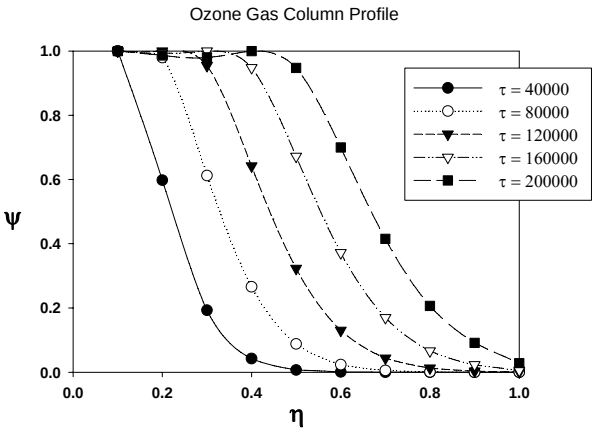

Figure 7. Normalized distribution of ozone gas in a column when St = 1, and Da_1= 1.

When the *St* and the Da_1 values both equal1, simulated column profiles shown in Figures 6 and 7 can be obtained. Under these conditions, the rates of interfacial mass transfer, convection, and chemical reaction are equal. Reactive zones of both VOC and ozone are effective across the column.

2. VOC and ozone breakthrough curves

Figure 8 below shows VOC and ozone breakthrough curves under the above three different conditions (i.e., $St << Da_1$, $St >> Da_1$, and $St = Da_1=1$). A general trend is observed that VOC remains a saturated concentration initially and then decreases, while ozone behaves vice versa. When $St << Da_1$, both the rates of reaction and convection are faster than mass transfer, implying that VOC and ozone would not exist simultaneously. In Figure 8, ozone breakthrough the column immediately after the VOC concentration drops to near zero. One can reasonably infer that once the ozone starts to exit the column, the NAPL in the column must have been completely removed. An entirely different phenomenon can be observed when $St >> Da_1$ (i.e., St = 100, and Da_1 = 0.01 in Figure 8). It is seen that under such condition the VOC still remains saturated when ozone completely breaks through the column. Recall that this is a condition when the rate of mass transfer is greater than both convection and reaction. Therefore, VOC is kept saturated in most sections of the column (see Figure 4) as well as at the exit. For ozone, even when the concentration is at its maximum (i.e., the inlet concentration) in the column VOC can still remains saturated due to a very slow rate of reaction. From this observation, one should avoid applying a high flow rate under this condition in order to save the ozone cost.

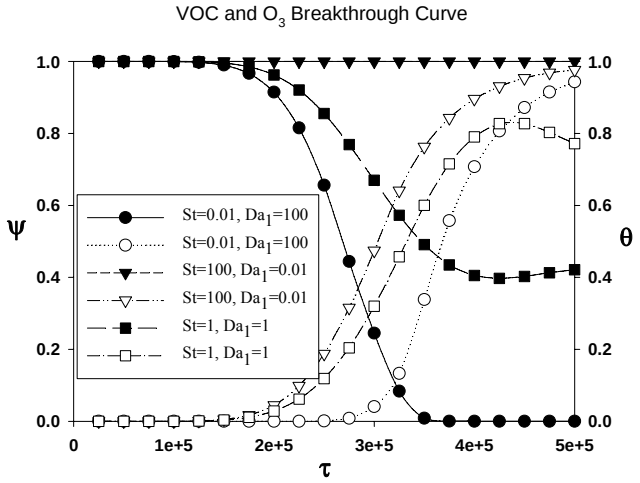

Figure 8. VOC and ozone breakthrough curves (BTCs) under various Stanton and Damkohler numbers. Solid and open symbols represent the VOC (θ) and ozone (Ψ) concentrations, respectively.

3. Ozonation of NAPL-Contaminated Soil Column

Figure 9 below shows results of venting experiments using N_2 gas alone. This is , in fact, the condition to mimic soil vapor extraction (SVE). It was observed that the toluene vapor concentration gradually increased within 5 minutes and then maintained at a saturated concentration of about 23 ppm for 20 minutes before it slowly decreased to a minimum at 60 minutes. However, when the O_3 gas was applied, significantly different toluene breakthrough curves (BTCs) were observed. Figure 10 demonstrates results when O_3 was injected to the identical column as in Figure 9. It was seen that at the initial 5 minutes there was no breakthrough concentration of toluene. This is because toluene is consumed by O_3 through gas phase reactions. Although toluene also reached the peak concentration of 23 ppm, the duration is much shorter due to chemical reactions. The benefit of adding O_3 to the system was that the total amount of toluene vapor was reduced due to reaction as can be seen by comparing areas under the toluene BTCs, which represent the total mass of toluene vapor. In addition, O_3 breaks through the column at almost the time as toluene and gradually reached the inlet concentration at about 30 minutes.

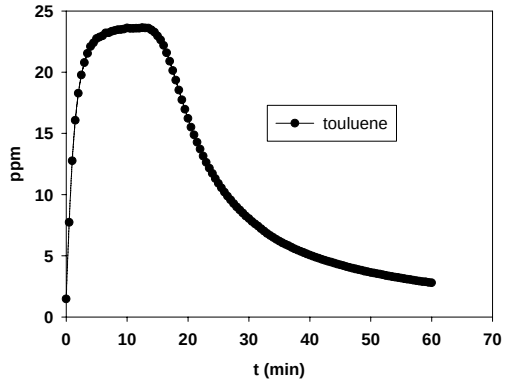

Figure 9. BTC of toluene vapor. Experimental conditions: O_3 flow rate = 150 mL/min, volume of toluene liquid = 0.5 mL, and the location of toluene is in the middle of the column.

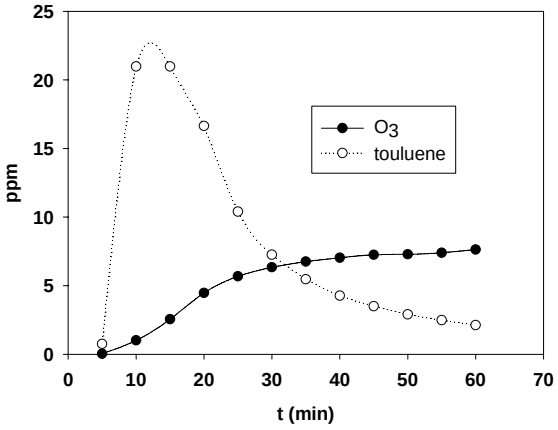

Figure 10. O_3 and toluene BTCs. Experimental conditions are as below: O_3 concentration = 7 ppm, O_3 flow rate = 150 mL/min, volume of toluene liquid = 0.5 mL, and the location of toluene is in the middle of the column.

Figures 11 and 12 are results conducted under different O_3 flow rates of 200 and 50 mL/min, respectively. It is seen from Figure 11 that at a higher flow rate of ozone (compared to 150 mL/min) both toluene vapor and O_3 would exit the column at a faster rate. The effects of flow rate become significant when the flow rate reduces to

50 mL/min as shown in Figure 12, where the toluene vapor concentration reached saturation after 100 minutes and the O_3 did not exit the column until 50 minutes. From results of three different flow rates, it is evident that the maximum toluene concentration is not dependent on flow rate. This implies that the liquid to vapor mass transfer rate of toluene is much faster than the rate of gas-phase chemical reaction. Therefore, toluene vapor always has time to accumulate before it reacts with O_3 and the only effective method to increase the removal efficiency is to increase the O_3 concentration.

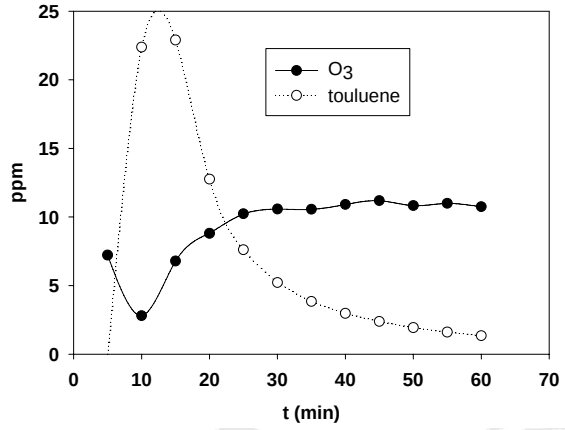

Figure 11. BTC of toluene vapor. Experimental conditions: O_3 flow rate = 200 mL/min, volume of toluene liquid = 0.5 mL, and the location of toluene is in the middle of the column.

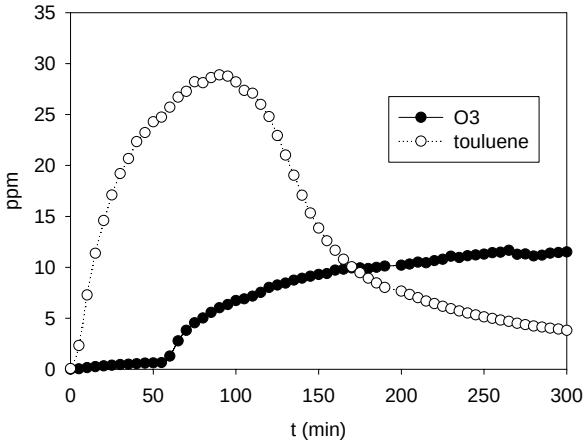

Figure 12. O_3 and toluene BTCs. Experimental conditions are as below: O_3 concentration = 7 ppm, O_3 flow rate = 50 mL/min, volume of toluene liquid = 0.5 mL, and the location of toluene is in the middle of the column.

The above were results of the condition when the toluene liquid (0.5 mL) was spiked in the middle of the column. We also conducted experiments when toluene liquid (2 mL) was spread uniformly in a column. Figure 13 shows results of BTCs under such conditions at a flow rate of 150 mL/min. It is evident that as the amount of toluene increases the time to remove the toluene increases significantly. The duration of toluene saturation was about 150 minutes. However, as in previous cases O_3 starts to exit the column when toluene vapor is still saturated, implying a mass transfer controlled process.

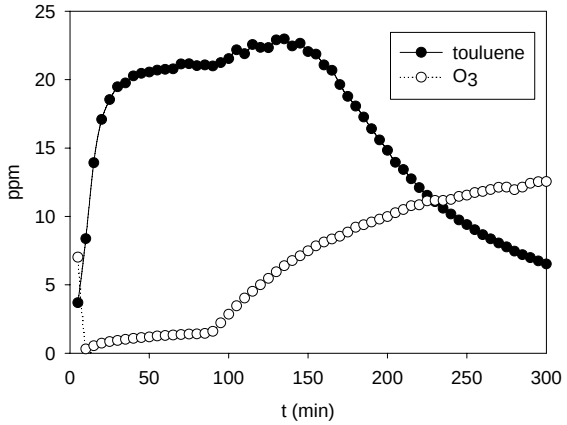

Figure 13. O_3 and toluene BTCs. Experimental conditions: O_3 concentration = 10 ppm, O_3 flow rate = 150 mL/min, volume of toluene liquid = 2 mL, and the toluene is spiked uniformly in the column.

V. Conclusions

The rate limiting step in the soil ozonation process for NAPL remediation can be determined using dimensionless variables, i.e., Stanton's and Damkohler's numbers, derived from this investigation. Both ozone and VOC column profiles under various rates of interfacial mass transfer, convection, and chemical reaction can be obtained to understand profile behaviors. The simulated results revealed that the process can be most efficiently operated when the rate of reaction is much faster than the rate of mass transfer (e.g., St = 0.01, and $Da_l = 100$). In laboratory soil column experiments, it was found that by injecting ozone gas into the column the overall removal rate of NAPL can be enhanced. In the case of toluene, it was observed that when different ozone flow rates were applied the saturated vapor concentration remains the same, indicating a mass transfer control process. The overall rate of removal can be increased by increasing ozone gas concentration.

VI. References

Harper, B. M., W. H. Stiver, et al. (2003). "Nonequilibrium nonaqueous phase liquid mass transfer model for soil vapor extraction systems." Journal Of Environmental Engineering-ASCE **129**(8): 745-754.

Hayden, N. J., T. C. Voice, et al. (1994). "Change in Gasoline Constituent Mass-Transfer during Soil Venting." J. Environ. Eng. - ASCE **120**: 1598-1641.

Ho, C. K., Liu S. W. et al. (1994). "Propagation of Evaporation and Condensation

Fronts during Multicomponent Soil Vapor Extraction." Journal of Contaminant Hydrology **16**: 381-401.

Khachikian, C. and T. C. Harmon (2000). “Long-term studies on the effects of nonvolatile organic compounds on porous media surface areas” J. of Environ. Quality **31** (4): 1309-1315, 2002

Mercer, J. W. (1990). “A review of immiscible fluids in the subsurface: Properties, models, characterization and remediation“ J. Contam. Hydrol. **6**: 107-163.

Rogers, S. W. and S. K. Ong (2000). "Influence of Porous Media, Airflow Rate, and Air Channel Spacing on Benzene NAPL Removal during Air Sparging." Environ. Sci. Technol. **34**: 764-770.

Shin, W. T., X. Garanzuay, et al. (2004). "Kinetics of soil ozonation: an experimental and numerical investigation." Journal Of Contaminant Hydrology **72**(1-4): 227-243.

Sung, M. H. and C. P. Huang (2002). "In situ removal of 2-chlorophenol from unsaturated soils by ozonation." Environmental Science & Technology **36**(13): 2911-2918.

Yoon, H., J. H. Kim, et al. (2002). "Effect of water content on transient nonequilibrium NAPL-gas mass transfer during soil vapor extraction." J. Contam. Hydrol. **54**: 1-18.

VII. 計畫成果自評

本研究依照原計畫進度，達成模擬與實驗之結果，這將對污染廠址應用臭氧處理法之可行性評估以及處理效率之模擬等有決定性的影響。本研究成果在做最後之綜合整理與分析後，將投稿於相關學術期刊。